Active Control of Surface Plasmonics with Ferroelectricity

ARTICLE · MARCH 2010

READS
21

10 AUTHORS, INCLUDING:

Maria Claudia Troparevsky
University of Tennessee
15 PUBLICATIONS **284** CITATIONS
SEE PROFILE

Katyayani Seal
Oak Ridge National Laboratory
41 PUBLICATIONS **376** CITATIONS
SEE PROFILE

Baohua Gu
Oak Ridge National Laboratory
160 PUBLICATIONS **6,690** CITATIONS
SEE PROFILE

Zhenyu Zhang
University of Science and Technology of China
362 PUBLICATIONS **7,338** CITATIONS
SEE PROFILE

NANO LETTERS

LETTER

pubs.acs.org/NanoLett

High Tunability of the Surface-Enhanced Raman Scattering Response with a Metal−Multiferroic Composite

Xiaoying Xu,[†] Katyayani Seal,[∥] Xiaoshan Xu,[†] Ilia Ivanov,[‡] Chun-Hway Hsueh,[⊥,∥] Nahla Abu Hatab,[§] Lifeng Yin,[#] Xiangqun Zhang,[▽] Zhaohua Cheng,[▽] Baohua Gu,[§,∥] Zhenyu Zhang,[∥,¶] and Jian Shen*[,#,∥]

[†]Materials Science and Technology Divisions, [‡]Center for Nanophase Materials, and [§]Environmental Sciences Division, Oak Ridge National Laboratory, Oak Ridge, Tennessee 37831, United States

[∥]Department of Physics and Astronomy, University of Tennessee, Knoxville, Tennessee 37996, United States

[⊥]Department of Materials Science and Engineering, National Taiwan University, Taipei 106, Taiwan

[#]Department of Physics, Fudan University, Shanghai 200433, China

[▽]Institute of Physics, Chinese Academy of Sciences, Beijing 100190, China

[¶]ICQD/HFNL, University of Science and Technology of China, Hefei, Anhui, 230026, China

ABSTRACT: We demonstrate active control of the plasmonic response from Au nanostructures by the use of a novel multiferroic substrate—$LuFe_2O_4$ (LFO)—to tune the surface-enhanced Raman scattering (SERS) response in real time. From both experiments and numerical simulations based on the finite-difference time-domain method, a threshold field is observed, above which the optical response of the metal nanostructure can be strongly altered through changes in the dielectric properties of LFO. This offers the potential of optimizing the SERS detection sensitivity in real time as well as the unique functionality of detecting multiple species of Raman active molecules with the same template.

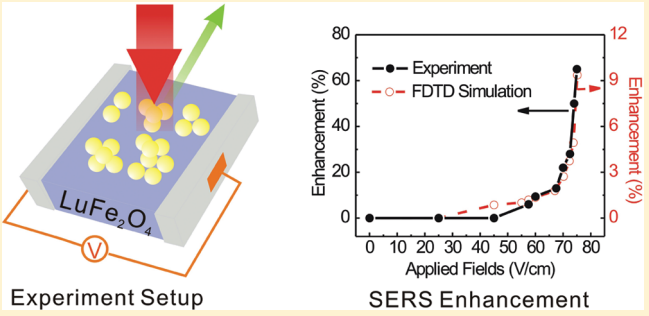

KEYWORDS: Tunable SERS, FDTD simulation, multiferroic, $LuFe_2O_4$

Surface-enhanced Raman scattering (SERS) has evolved as one of the most sensitive spectroscopic techniques for label-free chemical and biological detection.[1] SERS enhancement factors are a result of the strong local fields from the intrinsic plasmon resonances of metal nanoparticles coupling with the electronic transition resonances within the molecule. The ultrahigh sensitivity attributable to SERS is maximized when the plasmon resonance wavelength falls in between the excitation wavelength of the molecular resonance and the Stokes-shifted wavelength.[1] While the plasmon resonance wavelength depends strongly on the size, shape, composition, orientation, and dielectric environment of the metal nanostructure,[1−9] it is an arduous task to precisely adjust the nanostructure geometry, particularly the nanogap size designed for a specific molecular species and excitation wavelength where local electric field enhancement occurs.[10−16] As a result, although sensitivities up to the single molecule level have been observed via SERS, this has been restricted to some randomly oriented nanoparticles within a specific SERS template where limited numbers and species of molecules can be detected.[1,17−19] To date, few SERS templates have the tunability with respect to the gap and molecular size necessary to achieve maximal SERS enhancement.[20] In this regard, it is extremely advantageous to have a single yet tunable SERS template for an optimal plasmonic response over a range of wavelengths for the detection of multiple molecules. Such a template also enables optimal coupling of the plasmon resonance with different molecular resonances within the same molecule.

Recent efforts have demonstrated real-time influence on the plasmonic response of SERS templates by changing the interparticle distance, a critical parameter in template design,[6,14−16] through thermal expansion of polymer substrates.[15] However, inducing changes by this method was found to be relatively slow, irreversible and subject to specific moisture content. Further work has involved the use of laser tweezers to control the interparticle distance and influence the SERS response.[14] However this method is obviously not practical for real-world SERS applications. Hitherto unexplored in the context of SERS applications, an equally important and, arguably, equivalent method of controlling the plasmonic (or SERS) response of a metal template is through varying the dielectric properties of the substrate that adjoins the metal nanostructure, instead of the interparticle distance. Recent related work has successfully demonstrated the application of high external electric fields on electro-optic substrates to vary the dielectric constant for active tuning of the plasmonic response.[21,22]

Received: December 8, 2010
Revised: February 4, 2011
Published: February 15, 2011

Here we report the first demonstration of complete (reversible) active control of the Raman response of a plasmonic system, with the potential of an extremely high modulation response at modest applied biases. This is achieved by using a novel multiferroic substrate of increasing prominence—Lu-Fe_2O_4 (LFO)—to tune the SERS response of an Au nanostructure in real time. A clear threshold field is observed, above which the plasmonic response of the metal nanostructure can be strongly altered through changes in the dielectric properties of LFO thus demonstrating a high degree of tunability. The unique Fe-ion mixed valence that results from the Fe−O triangular lattice of LFO leads to large dielectric constants and also to ferroelectric behavior that is attributed to electronic charge ordering[23−29] instead of the pairing of anion and cation—which is the case for conventional ferroelectrics. Therefore, this material promises larger and faster changes in dielectric constant (and refractive index) at dc applied bias fields that are tens of volts/cm and, thus, several orders of magnitude lower than in conventional electro-optic materials used in recent related work.[21,22] For SERS applications, LFO based templates can enable active tuning of the SERS response to optimize the detection sensitivity in real time as well as the unique functionality of detecting multiple species of Raman active molecules with the same template.

Colloidal Au nanoparticles (30 nm) sorbed with thionine molecules as a Raman probing molecule were placed on top of the LFO substrate and air-dried to form Au clusters on the surface. Metallic clusters, especially those that display self-similar geometry, have been identified as one of the most favorable morphologies for high field enhancement,[1−3,5] through the use of which dramatically high Raman enhancement factors resulting in single molecule sensitivity have been reported.[17−19] Figure 1a shows a scanning electron microscope (SEM) image of one of the Au clusters aggregates. The clusters are sparsely distributed on the substrate (intercluster distance >5 μm) and their average size can vary from submicrometer to a few micrometers.

Silver electrodes that were 4 mm long were placed 2 mm apart on the substrate in order to apply a voltage bias. As shown in Figure 1b, the applied field across the electrodes induces a change in the dielectric constant of the LFO substrate, and the resulting change in the plasmonic response is characterized by measuring the scattered Raman signal from the Au clusters. Reflectivity spectra of these samples were measured at room temperature using a Cary 5000 spectrophotometer with a spot size of 1 × 2 mm. All SERS measurements were carried out with a Renishaw micro-Raman system spectrometer at an excitation wavelength of 785 nm with Thionine dye as the analyte. The integration time for each spectrum was 10 s, and the laser power was about 1 mW at the exit of the microscope objective. The spot size of the incident laser is about 2 μm, and thus by choosing appropriate Au clusters, measurements were limited to a single cluster.

Figure 2a shows the reflectivity of Au clusters with wavelength, which shows an absorption peak around 980 nm. Due to the large spot size of the light source, the measurement is made over several Au clusters, resulting in a broadened peak. In panels b and c of Figure 2 the real and imaginary parts of the refractive index of bare LFO are plotted. These data were obtained through Kramers−Kronig analysis by fitting the experimental reflectivity data. All the data are normalized by the refractive index value at 0 V/cm in order to show a clear trend in the spectra when a voltage is applied. The details of the spectra at 0 V/cm can be found in ref 30. The index change $|\Delta n| = 0.04$ (2% relative change) at an electric field of 75 V/cm at the wavelength of 785 nm. In

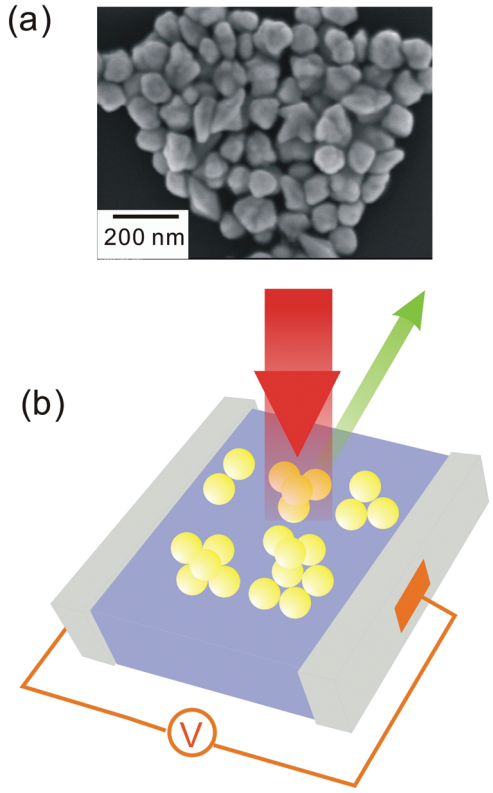

Figure 1. (a) Scanning electron micrograph of a cluster of aggregated Au nanoparticles on the LFO substrate. (b) A schematic illustration of the experiment setup with an in-plane applied voltage.

comparison, in order to have a similar effect of $\Delta n = 0.03$, an electrical field as high as 7.5×10^5 V/cm (which is above the coercive field) is needed for the BaTiO3 substrate in ref 21. The change in reflectivity in our experiment originates from the unique layered structure of multiferroic LFO. Spontaneous polarization in LFO is induced by the 3D charge ordering of Fe^{2+} and Fe^{3+} ions in the Fe oxygen double layer (W layer).[24] Upon the application of an electrical field ranging from 25 to 75 V/cm (5 to 15 V), the charge ordered state is gradually broken down, which manifests itself as a change in the dielectric constant of the LFO substrate. The altered dielectric environment of the metal clusters then results in a change in their plasmonic response (reflectivity). Figure 2d shows the changes in n and k for bare LFO at a wavelength of 785 nm as functions of the applied field. Above a threshold value of ~60 V/cm, the changes in the dielectric constant and consequently the plasmonic response are increasingly strong.

Figure 3a is a plot of the Raman spectrum of Au clusters on LFO over a wavenumber range of 300 to 1800 cm^{-1} at applied fields of 75 and 0 V/cm. Peak area from the SERS spectra of the thionine centered at 1123 cm^{-1} which corresponds to the out-of-plane C−H stretching is the focus of this data analysis. In order to show the reversibility and repeatability of Raman enhancement, several measurements alternating between 0 V/cm and the peak applied field 25, 60, or 75 V/cm were repeated and the relative area under the peak is plotted in Figure 3b. This repeatability of the experiment cycles is also desirable to avoid photodegradation effects although only about 1 mW of the laser power was used in the measurement. The minimum values of each curve, which correspond to peak area at 0 V/cm, are manually

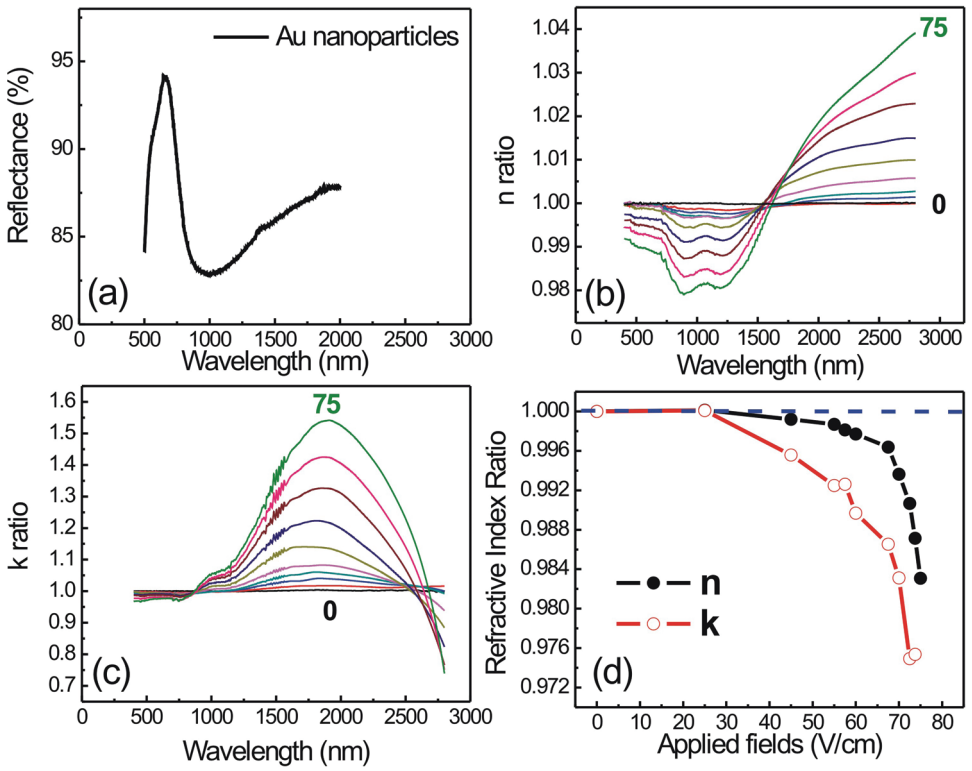

Figure 2. (a) Reflectance of Au clusters on $LuFe_2O_4$ at 0 V/cm. (b) Real and (c) imaginary parts of the refractive index of the bare $LuFe_2O_4$ substrate relative to 0 V/cm. (d) Relative changes of n and k values at different applied electric fields at a wavelength of 785 nm.

offset to provide a comparison of the changes in the peak area with bias. The variation of the peak area with voltage is repeatable over several cycles. This demonstrates the robustness of the LFO substrate as well as the metal nanostructures and, more critically, the reversibility of the bias controlled response, an important feature for device applications. We do not observe any hysteresis effects during the reversal of the applied field since it is well below the coercivity of LFO at room temperature.[27] In order to separate the pure plasmonic response of the Au clusters from the applied bias, we deposited colloidal nanoparticles on SiC and glass substrates and measured the reflectivity and Raman spectra with applied bias. No changes were observed in these samples. This implies that the variations in the Raman response of the system with applied bias originate predominantly from the consequent refractive index changes of the LFO substrate. Thus, pure electronic or other phenomena that may result as a response to the applied fields are not dominant and not evident in the data.

As shown in Figure 4a, for applied bias at and above ~60 V/cm the peak area increases with applied bias and can be as high as 65% at 75 V/cm. However, the SERS enhancement is reduced by ~4% due to the reduced local electric field on the LFO surface when a voltage is applied. Below 60 V/cm, the changes in the peak area are negligible. Thus, a threshold behavior is evident, with an onset at 60 V/cm similar to the reflectivity profile of the LFO substrate. Above this value, the Raman enhancement increases dramatically with increase in applied field. This threshold behavior, which originates from anomalous charge ordering behavior, is unique to LFO and provides the rare advantage of enabling extremely large changes in the dielectric constant for applied fields above the 60 V/cm threshold. From previous studies on LFO,[24,25,28] the possibility of applying higher fields up to 200 V/cm at room temperature, and even much higher at lower temperatures, has been successfully demonstrated in LFO. For LFO stoichiometries similar to the one used in the current experiment, the measured coercive field and the subsequent change in the polarization are significantly high.[25,28] This suggests that the tunability of the dielectric constant of LFO and the resulting plasmonic response can be extended up to an order of magnitude beyond the range estimated in the current work, making it a truly powerful and versatile control parameter in tunable SERS.

In order to simulate the experiment, numerical calculations based on the finite-difference time-domain (FDTD) method were performed. To compare the numerical results with experiment, the cross section of the Raman intensity, which is proportional to $|E|^4$, was estimated by obtaining the maximum local electrical field at a fixed wavelength of 785 nm. The refractive index values of the substrate were as per the experimental data n panels b and c of Figure 2. The substrate slab size was 0.1 × 0.1 μm and four close packed Au particles (diameter, 20 nm; intercluster spacing, <40 nm) were positioned on top of the substrate as shown in the inset of Figure 4b. The small intercluster gap effectively approximates the large cluster sizes in the experiment. The dielectric constants of gold were taken from Johnson and Christy[31] data. Periodic boundary conditions were employed in both x and y directions with nonuniform grid size. Specifically, the grid size was 0.5 nm in the vicinity of the gold nanoparticles and approximately 5 nm near the boundaries. As shown in Figure 4a, the local field intensity at 785 nm increases with the applied voltage bias. In this calculation, the structure was kept constant and the refractive index of the substrate was the only parameter that was varied for different voltages. As is evident from the two curves in Figure 4a, there is excellent qualitative agreement between experiment and numerical calculations for

dx.doi.org/10.1021/nl104291g |*Nano Lett.* 2011, 11, 1265–1269

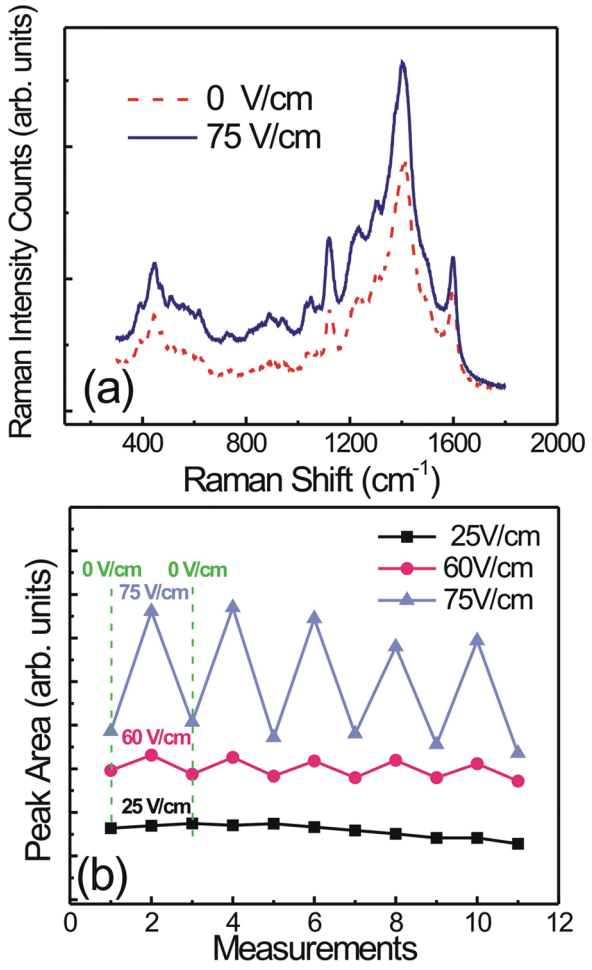

Figure 3. (a) SERS intensity changes at an applied bias of 75 V/cm. Red (dash) and blue (solid) lines correspond to SERS responses before and after applying a voltage. (b) SERS peak area at different fields with repeated cycles of applied bias.

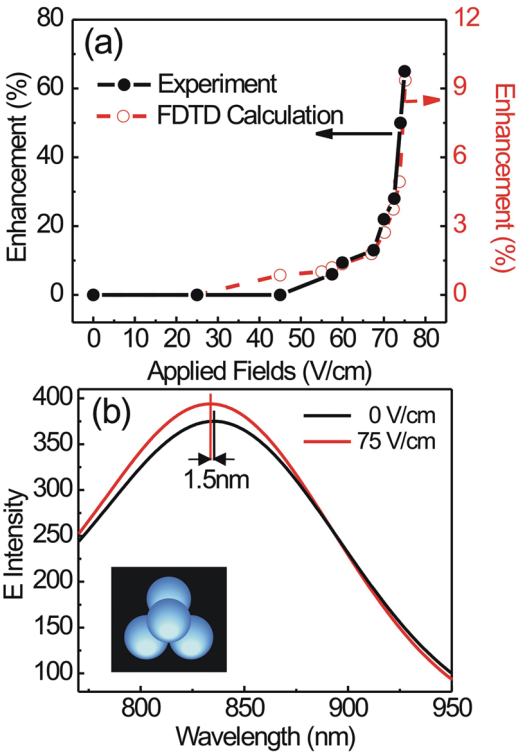

Figure 4. (a) Plot of Raman peak area vs applied fields from experiment (solid black line) and FDTD calculations (dashed red line) showing a threshold effect. (b) Blue shift in the local field $|E|^2$ with applied field obtained from calculations. The inset shows the Au cluster configuration.

the Raman intensity increase with the application of a bias voltage. The difference in the magnitude of the maximum enhancement between experiment and numerical calculations may be explained by the limitations of the accuracy of the FDTD calculations. These could include several factors such as system size limits and also due to the fact that the nanocluster sizes in the experiment are much larger than that used in calculation, vary significantly, and are not periodic in terms of their positions on the substrate. Some of the difference may also be attributed to the use of bulk values of the dielectric constant of gold in the calculation, which may introduce inaccuracies at the nanoparticle level. Additionally, environmental influences, chemical alteration of the substrate surface and gold nanoclusters, may be a factor. The qualitative agreements between the experimental results and the numerical estimates from FDTD suggest that the increase in the SERS signal at higher voltages is represented accurately by the simulations. This implies that the application of an applied field results in a local refractive index change in the LFO substrate which, in turn, is the primary mechanism for enabling the tuning or control of the optical response of the Au clusters, as verified through the Raman and reflectance data.

Our FDTD calculations indicate that the local field ratio increases with increase in cluster size and decrease in intercluster distance for periodically arranged clusters. This maximum is immediately decreased for an aperiodic structure but is fairly robust with small changes in the cluster size. These results confirm that the experimental Raman enhancement can be increased by using periodically positioned structures and optimal cluster configuration, as has been demonstrated in previous work in the field of SERS.[1,11−13]

Our numerical calculations also show a clear blue shift in the local field $|E|^2$ versus wavelength profile (shown in Figure 4b resulting from changes in the dielectric constant of LFO. The shift is about 1.5 nm with the application of a bias voltage as small as 75 V/cm and was found to be a robust feature despite changes in particle size and cluster configuration. A blue shift was also observed in the numerically obtained reflectance versus wavelength. Such shifts are not resolvable in the current experimental data due to the broad absorption peak of our metal clusters. In the future, the use of periodic structures with narrow reflection spectra and the use of higher voltages should allow for observable shifts in the experiment. The spectral shift demonstrated in the calculations is a critical advantage in the application of tuning the Raman response of plasmonic nanostructures to detect multiple species of molecules with the same template. To fully capitalize on this application, we envision the use of metal nanostructure geometries that are already optimized for maximal SERS sensitivity (maximal field enhancement) with the added functionality of the dielectric tunability of an LFO substrate, resulting in potential spectral shifts of hundreds of cm^{-1}.[32]

For the first time, we demonstrate tunable plasmonic responses via SERS by applying electrical fields to a multiferroic substrate (LFO) with Au nanoclusters. The estimated refractive index change is of the order of magnitude of related work[21] even

dx.doi.org/10.1021/nl104291g |*Nano Lett.* 2011, 11, 1265–1269

at dramatically lower applied electric fields. The SERS enhancement is significant at ~65%. At the field strengths used, the electrical 3D charge ordering of the LFO substrate is gradually broken down, and the onset of which is evidenced by the threshold behavior of both the reflectivity as well as the SERS response of our samples at around 60 V/cm, which confirms that this behavior can predominantly be attributed to the refractive index changes in the substrate. FDTD calculations of this system suggest that the local refractive index change of the substrate accounts for the dominant portions of the Raman enhancement as well as the reflectivity. With the use of higher electrical fields through high-frequency pulsed voltage sources, one may anticipate a further increase in the field enhancement. This demonstration of repeatable and reversible changes in the optical response of the nanostructures paves the way for real-time active control and tuning of SERS templates for label-free chemical sensing. One can then conceive of sensing a wide variety of molecules with the same template. With the use of highly tunable LFO substrate, one can also anticipate a host of important applications, for example, controlling plasmon propagation via noble metal−LFO composites.[33] The electronic polarization characteristics of LFO indicate that one may also achieve high switching speeds[29] for device applications pertaining to the computing and communications industry. Enabling refractive index changes at low voltages also allows for the possibility of plasmonic circuitry at voltages that are within the realm of practical use.

AUTHOR INFORMATION

Corresponding Author
*E-mail: Shenj5494@fudan.edu.cn.

ACKNOWLEDGMENT

Research sponsored by the Laboratory Directed Research and Development Program of Oak Ridge National Laboratory, managed by UT-Battelle, LLC, for the U.S. Department of Energy (05315 and 00483). A portion of this research was conducted at the Center for Nanophase Materials Sciences, which is sponsored at Oak Ridge National Laboratory by the Scientific User Facilities Division, U.S. Department of Energy. C.H.H. acknowledges the partial support from National Science Council, Taiwan. L.F.Y and J.S. acknowledge the support from National Basic Research Program of China (973 Program) under the grant No. 2011CB921801.

REFERENCES

(1) Anker, J. N.; Hall, W. P.; Lyandres, O.; Shah, N. C.; Zhao, J.; Van Duyne, R. P. *Nat. Mater.* **2008**, *7*, 442.
(2) Stockman, M. I.; Pandey, L. N.; Muratov, L. S.; George, T. F. *Phys. Rev. Lett.* **1994**, *72*, 2486–2489.
(3) Shalaev, V. M. *Nonlinear Optics of Random Media: Fractal Composites and Metal-Dielectric Films*; Springer Tracts in Modern Physics, Vol. 158; Springer: Berlin and Heidelberg, 2000.
(4) Jensen, T. R.; Duval Malinsky, M.; Haynes, C. L.; Van Duyne, R. P. *J. Phys. Chem. B* **2000**, *104*, 10549–10556.
(5) Lee, S. J.; Morrill, A. R.; Moskovits, M. *J. Am. Chem. Soc.* **2006**, *128*, 2200–2201.
(6) Hatab, N. A.; Hsueh, C.-H.; Gaddis, A. L.; Retterer, S. T.; Li, J.-H.; Eres, G.; Zhang, Z.; Gu, B. *Nano Lett.* **2010**, *10*, 4952–4955.
(7) Xu, Hongxing; Aizpurua, Javier; Käll, Mikael; Apell, Peter *Phys. Rev. E* **2000**, *62*, 4318.
(8) Xu, Hongxing; Bjerneld, Erik J.; Käll, Mikael; Börjesson, Lars *Phys. Rev. Lett.* **1999**, *83*, 4357.
(9) Xu, Hongxing; Käll, Mikael *Sens. Actuators, B* **2002**, *87*, 244.
(10) Stuart, D. A.; Yonzon, C. R.; Zhang, X.; Lyandres, O.; Shah, N. C.; Glucksberg, M. R.; Walsh, J. T.; Van Duyne, R. P. *Anal. Chem.* **2005**, *77*, 4013–4019.
(11) Perney, N. M. B.; García de Abajo, F. J.; Baumberg, J. J.; Tang, A.; Netti, M. C.; Charlton, M. D. B.; Zoorob, M. E. *Phys. Rev. B* **2007**, *76*, No. 035426-1−5.
(12) Mahajan, S.; Abdelsalam, M.; Suguwara, Y.; Cintra, S.; Russell, A.; Baumbergb, J.; Bartlett, P. *Phys. Chem. Chem. Phys.* **2007**, *9*, 104–109.
(13) Alvarez-Puebla, R.; Cui, B.; Bravo-Vasquez, J.; Veres, T.; Fenniri, H. *J. Phys. Chem. C* **2007**, *111*, 6720–6723.
(14) Svedberg, F.; Li, Z.; Xu, H.; Kall, M. *Nano Lett.* **2006**, *6*, 2639–2641.
(15) Lu, Y.; Liu, G. L.; Lee, L. P. *Nano Lett.* **2005**, *5*, 5–9.
(16) Persson, B. N. J.; Zhao, K.; Zhang, Z. *Phys. Rev. Lett.* **2006**, *96*, No. 207401−4.
(17) Nie, S.; Emory, S. R. *Science* **1997**, *275*, 1102–1106.
(18) Dieringer, J. A.; Ii, R. B. L.; Scheidt, K. A.; Van Duyne, R. P. *J. Am. Chem. Soc.* **2007**, *129*, 16249–16256.
(19) Kneipp, K.; Wang, Y.; Kneipp, H.; Perelman, L. T.; Itzkan, I.; Dasari, R. R.; Feld, M. S. *Phys. Rev. Lett.* **1997**, *78*, 1667–167.
(20) Alexander, Kristen D.; Skinner, Kwan; Zhang, Shunping; Wei, Hong; Lopez, Rene *Nano lett.* **2010**, *10*, 4488–4493.
(21) Dicken, M. J.; Sweatlock, L. A.; Pacifici, D.; Lezec, H. J.; Bhattacharya, K.; Atwater, H. A. *Nano Lett.* **2008**, *8*, 4048–4052.
(22) Dickson, W.; Wurtz, G. A.; Evans, P. R.; Pollard, R. J.; Zayats, A. V. *Nano Lett.* **2008**, *8*, 281–286.
(23) Subramanian, M. A.; He, T.; Chen, J.; Rogado, N. S.; Calvarese, T. G.; Sleight, A. W. *Adv. Mater.* **2006**, *18*, 1737–1739.
(24) Li, C.; Zhang, X.; Cheng, Z.; Sun, Y. *Appl. Phys. Lett.* **2008**, *93*, No. 152103−6.
(25) Park, J. Y.; Park, J. H.; Jeong, Y. K.; Jang, H. M. *Appl. Phys. Lett.* **2007**, *91*, No. 152903−6.
(26) Ikeda, N.; Yamada, Y.; Nohdo, S.; Inami, T.; Katano, S. *Physica B* **1998**, *820*, 241–243.
(27) Yang, H. X.; Zhang, Y.; Ma, C.; Tian, H. F.; Qin, Y. B; Zhao, Y. G.; Li, J. Q. arXiv:0803.0819v2.
(28) Ikeda, N.; Ohsumi, H.; Ohwada, K.; Ishii, K.; Inami, T.; Kakurai, K.; Murakami, Y.; Yoshii, K.; Mori, S.; Horibe, Y.; Kito, H. *Nature* **2005**, *436*, 1136–1140.
(29) Ikeda, Naoshi *J. Phys.: Condens. Matter* **2008**, *20*, No. 434218.
(30) Xu, X. S.; Angst, M; Brinzari, T. V.; Hermann, R. P.; Musfeldt, J. L.; Christianson, A. D.; Mandrus, D; Sales, B. C.; McGill, S; Kim, J.-W; Islam, Z *Phys. Rev. Lett.* **2008**, *101*, No. 227602.
(31) Johnson, P. B.; Christy, R. W. *Phys. Rev. B* **1972**, *6*, 4370–4379.
(32) Kabashin, A. V.; Evans, P.; Pastkovsky, S.; Hendren, W.; Wurtz, G. A.; Atkinson, R.; Pollard, R.; Podolskiy, V. A.; Zayats, A. V. *Nat. Mater.* **2009**, *8*, 867.
(33) Li, Zhipeng; Bao, Kui; Fang, Yurui; Guan, Zhiqiang; Halas, Naomi J.; Nordlander, Peter; Xu, Hongxing *Phys. Rev. B* **2010**, *82*, No. 241402(R).